2019 IEEE 58th Conference on Decision and Control (CDC)
Palais des Congrès et des Expositions Nice Acropolis
Nice, France, December 11-13, 2019

Adaptive Impedance Control with Setpoint Force Tracking for Unknown Soft Environment Interactions

Trevor K. Stephens[1], Chaitanya Awasthi[1], Timothy M. Kowalewski[1]

Abstract— **Robots are often required to interact with surrounding environments to complete specific tasks. In these scenarios the robot must behave in a stable manner in both free-space motion as well as constrained motion during the interaction. Additionally, for many of these cases it is important to track a setpoint force to complete a task or provide safe interaction in the absence of typically expensive force sensors. This force tracking is fairly straightforward using impedance control if the environment is known exactly a priori. However, in practice the environment is unlikely to be known and force tracking becomes inaccurate. To overcome this problem we present an adaptive impedance controller with adaptation laws for the environment parameters derived directly from Lyapunov-based stability analysis. This work focuses on interactions with soft environments which are represented using a non-linear, viscoelastic Hunt-Crossley model. After derivation and stability analysis of the controller, we present simulations of a 1 degree of freedom (DOF) robot interacting with two distinct soft environments to demonstrate the efficacy of the controller.**

I. Introduction

Robots are increasingly used in a wide variety of applications. Many of these applications fall under motion control tasks, where the robot's position is controlled while moving through free-space. Other robotic tasks may require the robot to interact with surrounding environments. This is often called constrained motion, and is complicated by the interaction forces between the robot and environment. A proposed method to maintain safe interaction is impedance control introduced by Hogan [1]. In this control methodology, the impedance of the robot end effector is regulated throughout both free-space and constrained motions, as opposed to directly controlling either force or position. Although this method has been widely adopted, on its own impedance control does not have a mechanism for force tracking.

In this work we derive a Lyapunov-based adaptive impedance control to accomplish force tracking of robotic systems interacting with unknown environments. In this framework, we assume the functional form of the environment to be known, but the parameters describing the environment are initially unknown and are adapted online to achieve force tracking. We specifically present adaptive impedance control for a robot interacting with a soft, viscoelastic environment. This type of interaction is common in many domains and is of special interest in medical robotics, where robots interact with various tissues. These tissues are considered soft and viscoelastic and are modeled accurately using the Hunt-Crossley model [2]. Our approach for adaptive impedance control with force tracking derives adaptive laws directly from the proposed Lyapunov function and has the following appealing characteristics:

- Environment parameters are not needed to be known a priori
- Force tracking is achievable through estimation of environment parameters without the use of direct force measurement such as using a load cell
- Calculation of noise-prone, higher-order derivative terms, such as acceleration, is not necessary

The paper is outlined in the following manner: Section II describes background information pertinent to our work in constant force tracking for robots interacting with soft environments; Section III provides the derivation of the adaptive impedance controller; Section IV provides stability proof of the controller; Section V provides two simulation examples of a 1-DOF robot interacting with soft, viscoelastic environment with our proposed controller; Section VI provides simulated results of our controller; Section VII provides a discussion of the proposed work and the proposed benefits and limitations of this methodology; Section VIII concludes the paper with suggestions for future work and a summary of the work herein.

II. Background

A large portion of robot-environment interactions involve homogeneous and stiff environments, which are appropriately modeled by the heuristic Kelvin-Voigt model, which is linear, as shown in equation 1.

$$f_e = \begin{cases} k_e\delta + b_e\dot{\delta} & \delta \geq 0 \\ 0 & \text{otherwise} \end{cases} \tag{1}$$

Here, δ is the deformation into the tissue. This linear model accurately portrays many interactions, and is attractive due to its simplicity. Unfortunately, not all environments can be modeled with this spring-damper model, and require more complex models. A prime example is soft biological tissue. The non-linear, viscoelastic nature of tissue demands model terms to likewise incorporate non-linear, viscoelastic behavior; the Hunt-Crossley model is better suited to meet these requirements [3]. The model is shown in equation (2),

This material is based upon work supported in part by the National Science Foundation Graduate Research Fellowship under Grant No. 00039202. Any opinion, findings, and conclusions or recommendations expressed in this material are those of the authors and do not necessarily reflect the views of the National Science Foundation. (T. Stephens and C. Awasthi contributed equally to this work.) (Corresponding Author: C. Awasthi)

T. Stephens, C. Awasthi, and T. Kowalewski are with the Department of Mechanical Engineering, University of Minnesota, Minneapolis, MN, 55455 USA e-mail: (steph594@umn.edu, awast010@umn.edu, timk@umn.edu)

and introduces position-dependent damping to help overcome some of the shortcomings of the Kelvin-Voigt model.

$$f_e = \begin{cases} k_e\delta^n + b_e\delta^n\dot{\delta} & \delta \geq 0 \\ 0 & \text{otherwise} \end{cases} \quad (2)$$

Although the Hunt-Crossley model yields good fit to data [3], the non-linearities directly impact the complexity of estimating parameters online as well as controlling to a particular force during interactions.

Previous work has established successful attempts of impedance control with force regulation for a robot interacting with homogeneous, stiff environments. These environments are appropriately represented with the Kelvin-Voigt model in (1), or even more simply by a linear spring (i.e. $b_e = 0$ in (1)). For examples of impedance control with force tracking for these linear environments the reader is referred to [4], [5], [6], [7]. However, the same objective of controlling to a desired force when interacting with a soft, viscoelastic environment remains nascent. The most recent efforts in this area are described next.

Bhasin et al. early work in this area used adaptive control to regulate to a desired position during interactions with environments modeled using the Hunt-Crossley model [8]. The authors used a projection operator to derive adaptive laws. Stability was shown using Lyapunov method, but no extension using Barbalat's Lemma was shown, and therefore only boundedness was shown as opposed to asymptotic convergence. This early work does not show regulation to a given force and is not constructed in the framework of adaptive impedance control, but established initial work in the area of interaction with soft, viscoelastic environments.

Expanding on this initial work, Bhasin et al. propose a bounded neural network based controller to provide force limiting control during the interaction [9], [10]. This controller was composed of a bounded neural network term along with a saturated feedback term which in effect bounds the control input. The stability of this controller was also shown using Lyapunov method, but as before the controller did not regulate to a specific force, but rather limited the force to an upper bound. This was one step closer to force control as it at least guaranteed this bound.

A method for force tracking can be found in [11] which considers interactions with environments modeled using Hunt-Crossley model. The proposed method also uses a projection operator to derive the adaptation laws. The controller is set up as an impedance controller with a derived desired trajectory which results in the desired force in the steady-state. Knowledge of the exponential term, n, in (2) is required a priori. Also, the proposed controller requires knowledge of the environment force, which would require measurement through a sensor such as a load cell. The stability analysis is done using Lyapunov method, but asymptotic convergence is not shown. Simulations of the controller show accurate estimation of the environment parameter, k_e, as well as regulation to a desired force.

The previous methods for control were all adaptive controllers; a different approach is presented in [3]. Instead of adaptive control, this work utilized a Kalman filter based active observer to estimate tissue parameters online. To accomplish this, a first-order linearization of the Hunt-Crossley model was used. The linearization was done about a steady-state force value; due to this fact the controller performance degrades away from this linearization value and is not conducive to a large range of desired forces.

Along with the described controllers, other work has focused on techniques for parameter estimation without control. Initial work was reported in [12], where a two-stage estimation approach was proposed. Due to the non-linearity of the Hunt-Crossley model, the estimation was accomplished through two recursive least-squares (RLS) estimators interconnected via feedback. The RLS estimators were established based on a partial decoupling of parameters, with one RLS estimator estimating the stiffness (k_e) and damping terms (b_e), and the other RLS estimator estimating the exponential term (n). Although estimation was deemed accurate, simulation and experimental results show that this two-stage estimation technique is sensitive to initial parameters and suffers from a relatively slow convergence time as explained in [13]. These two shortcomings make this estimation technique unconducive to incorporate in a feedback control loop.

A single-stage estimation technique was proposed in [13] to alleviate the aforementioned problems with the two-stage approach. The single-stage estimation technique was accomplished by first linearizing the Hunt-Crossley model by taking the natural logarithm of both sides. This new linear-in-parameters model is conducive to RLS methods; the authors chose to utilize exponentially weighted recursive least squares (EWRLS) due to its advantages with estimating variable dynamic properties and faster convergence time. This single stage EWRLS approach was shown to be accurate, but has two potential shortcomings as pointed out by the authors. First, an approximation in regard to the natural logarithm function is used which relies on the assumption that the end effector speed is relatively small when in contact with the environment. This may be true in many cases, but is not easily guaranteed throughout the entire operation. The second limitation also is due to an approximation with the natural logarithm function, and requires that penetration must be "sufficiently" deep enough into the tissue. This requires that the estimator is only utilized once the robot has thoroughly penetrated the environment surface as detailed in [13]. This condition may prove limiting for control scenarios, because estimation can only start after sufficient penetration.

A more recent estimation approach was proposed in [14], where once again a two-stage identification approach was proposed. In contrast to the two-stage approach in [12], which suffered from slow convergence time and high sensitivity to initial parameters, this two-stage approach is not interconnected via a feedback loop, and therefore does not suffer from these same limitations. Instead, this two-stage approach first utilizes a Quad-Poly model linearly parameterized for use with EWRLS. The parameter estimates from this first stage are then used in a lookup table to

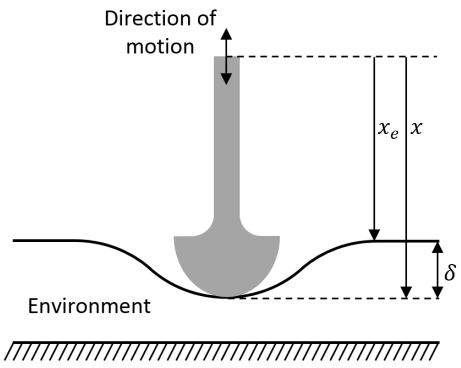

Fig. 1. Schematic of 1-DOF interaction with environment

identify the exponential term, n. Given knowledge of the parameter n, the stiffness (k_e) and damping (b_e) are linearly parameterized and the second stage concludes with EWRLS to estimate these two parameters. This full approach is called two-stage polynomial identification (TSPI), and was found to be more accurate than the previously proposed log-linearization approach. Specifically, TSPI far exceeded the log-linearization approach in contact regions close to the environment boundary, because TSPI does not rely on any assumptions regarding sufficient penetration into the environment.

These approaches all provide estimation of Hunt-Crossley model parameters without regard to control. By combining any of these estimators within a control scheme, a separate analysis would be necessary to guarantee stability of the combined controller and estimator. Additionally, each of the estimation techniques mentioned require the use of force estimation through sensors such as load cells. This may not be conducive in many applications, and are especially challenging in medical scenarios [15], [16]. These reasons motivate our proposed work of adaptive impedance control with force tracking.

III. Adaptive Impedance Control

As mentioned previously, an impedance controller can be used for force tracking in a known environment. However, it does not have a mechanism for force tracking in an unknown environment. On the other hand, an adaptive controller can be used for estimating parameters of an unknown environment (assuming a known form for the environment), but it does not have a mechanism for force tracking. To address this problem, we now present an adaptive impedance controller. Table I defines the various symbols used throughout this derivation.

A. Modeling and Notation

In this work we consider robot dynamics of the form:

$$m\ddot{x} + b\dot{x} = F_{in} - F_e \tag{3}$$

where m and b are robot mass and damping, respectively. The state, x, represents position of the robot end effector with $\dot{x}$ representing velocity and $\ddot{x}$ representing acceleration. The state, x, is assumed measurable with its derivatives accessible through numerical differentiation. The dynamics of the robot are based on the model of a DC motor with 1 degree of freedom (DOF). However, the adaptive impedance controller derived in this work can be generalized to multiple DOFs. The controller input force is denoted by F_{in} and the environment force is denoted by F_e. The robot is assumed to be interacting with soft environments, such as tissue, where the environment force is represented using the Hunt-Crossley model as explained previously and restated here:

$$F_e = \begin{cases} k_e\delta^n + b_e\delta^n\dot{\delta} & \delta \geq 0 \\ 0 & \text{otherwise} \end{cases} \tag{4}$$

where δ is taken as the deformation of the tissue and is defined in (5). Additionally, $\dot{\delta}$ is the relative rate of deformation of the tissue. The terms k_e and b_e are tissue stiffness and damping parameters, respectively. The exponential term, n, is the Hertzian compliance coefficient, and is usually assumed to be between 1 and 2. For this work, it was assumed constant at 1.8 similar to assumptions made in [11].

$$\delta = \begin{cases} x - x_e & x > 0 \\ 0 & \text{otherwise} \end{cases} \tag{5}$$

Here, x_e represents the tissue boundary as shown in Figure 1 and is measured from the same frame of reference as x. The value of x_e is assumed to be known and constant.

B. Controller Derivation

We begin the derivation by selecting a value for F_{in} to obtain a desired impedance model:

$$F_{in} = mM_t^{-1}(-B_t\dot{e} - K_te + \gamma) + \hat{F}_e + b\dot{x} \tag{6}$$

Here, M_t, B_t, and K_t represent target inertia, damping, and stiffness impedance parameters, respectively. The interaction between the robot and the environment is modeled as a 2^{nd} order mass-spring-damper system, and the value of the impedance parameters are chosen so as to shape the interaction (overdamped, critically damped, etc.). In this way, we obtain a desired impedance model. The terms e and $\dot{e}$ represent the error and its derivative, respectively, where error is defined as $e = x - x_r$. The expression for x_r will be defined later, which is the reference trajectory used to drive the actual force to a desired force, F_d. Additionally, γ is a placeholder term to be defined later which helps facilitate stability analysis. The term $\hat{F}_e$ denotes an estimate of F_e. This hat notation is adopted throughout the paper to likewise signify an estimate.

We substitute the value of F_{in} as defined in (6), to the dynamic model in (3):

$$m\ddot{x} + b\dot{x} = mM_t^{-1}(-B_t\dot{e} - K_te + \gamma) + \hat{F}_e + b\dot{x} - F_e \tag{7}$$

After algebraic simplification, (7) can be expressed as the following:

TABLE I
DEFINITION OF SYMBOLS

Symbol	Definition
m, b	Mass and damping terms of the robot model
x, $\dot{x}$, $\ddot{x}$	Position, velocity, and acceleration of robot (see Figure 1)
x_e	Position of environment (see Figure 1)
δ, $\dot{\delta}$	Deformation and deformation rate of environment (see Figure 1 and Equation 5)
F_e	Environment force (see Equation 4)
F_{in}	Controller input force (see Equation 6)
M_t, B_t, K_t	Target mass, damping, and stiffness parameters for the impedance controller
γ	Placeholder term used within the expression for F_{in} (see Equation 12)
$\hat{F}_e$	Estimate of environment force
$\tilde{F}_e$	Difference between actual and estimated environment force (i.e. $F_e - \hat{F}_e$)
x_r	Feasible online reference trajectory (see equation 28)
x_r^*	Ideal reference trajectory (see equation 27)
e	Error between robot position and feasible online reference trajectory (i.e. $x - x_r$)
σ	Sliding surface like term to facilitate stability analysis (see Equation 9)
k_e, b_e	Stiffness and damping terms in Hunt-Crossley environment model
$\hat{k}_e$, $\hat{b}_e$	Estimate of stiffness and damping terms in Hunt-Crossley environment model
$\tilde{k}_e$, $\tilde{b}_e$	Estimation error in stiffness and damping terms in Hunt-Crossley environment model
$\dot{\hat{k}}_e$, $\dot{\hat{b}}_e$	Derivative terms for stiffness and damping estimates in Hunt-Crossley environment model (see Equations 22 and 23)

$$M_t\ddot{x} + B_t\dot{e} + K_t e = \gamma - m^{-1}M_t\tilde{F}_e \tag{8}$$

Here, $\tilde{F}_e = F_e - \hat{F}_e$ is defined as the difference in actual and estimated environment forces, with the tilde symbol used throughout the paper in this manner.

To facilitate stability analysis, a sliding surface like term, σ, is chosen as follows:

$$\sigma = M_t\dot{x} + B_t e \tag{9}$$

Note, the objective of constructing σ is to use it in stability analysis of the adaptive impedance controller and to show that σ asymptotically approaches zero, with the ultimate goal of driving the error, e, asymptotically to zero. Since (9) is a mixed differential equation, σ approaching zero does not necessarily guarantee that e is also driven to zero, however it will be later shown that this is indeed the case.

We take the derivative of (9) to obtain:

$$\dot{\sigma} = M_t\ddot{x} + B_t\dot{e} \tag{10}$$

By combining (8) with (10) we obtain the following:

$$\dot{\sigma} = -K_t e + \gamma - m^{-1}M_t\tilde{F}_e \tag{11}$$

Now, we can strategically select γ to cancel out the $K_t e$ term as well as provide a useful term for stability analysis:

$$\gamma = -K\sigma + K_t e \tag{12}$$

where, K is selected as a positive gain. At this point, Lyapunov stability analysis can be conducted.

IV. STABILITY ANALYSIS

Theorem: *The controller given by (6) guarantees setpoint force tracking, i.e., $F_e \to F_d$ if $x \to x_r^*$ as $t \to \infty$.*
Assumption: We assume that the tissue deformation, δ, is bounded from above, due to geometry of the robot.

Proof. The proof of the theorem is broken down into five parts for ease of following.

A. Lyapunov Stability

We start by defining a candidate Lyapunov function with α and β as positive scalars:

$$V(\sigma, \tilde{k}_e, \tilde{b}_e) = \frac{1}{2}\sigma^2 + \frac{1}{2}\alpha\tilde{k}_e^2 + \frac{1}{2}\beta\tilde{b}_e^2 \tag{13}$$

With the derivative of (13) being computed as follows:

$$\dot{V} = \sigma\dot{\sigma} + \alpha\tilde{k}_e\dot{\tilde{k}}_e + \beta\tilde{b}_e\dot{\tilde{b}}_e \tag{14}$$

Substituting (11) and (12) into (14) we obtain:

$$\dot{V} = \sigma(-K\sigma - m^{-1}M_t\tilde{F}_e) + \alpha\tilde{k}_e\dot{\tilde{k}}_e + \beta\tilde{b}_e\dot{\tilde{b}}_e \tag{15}$$

The expression for $\tilde{F}_e$ can be written as follows:

$$\tilde{F}_e = \delta^n(\tilde{k}_e + \tilde{b}_e\dot{\delta}) \tag{16}$$

By simplifying (15) and substituting in (16) we obtain:

$$\dot{V} = -K\sigma^2 - \tilde{k}_e(m^{-1}M_t\sigma\delta^n - \alpha\dot{\tilde{k}}_e) - \tilde{b}_e(m^{-1}M_t\sigma\delta^n\dot{\delta} - \beta\dot{\tilde{b}}_e) \tag{17}$$

Here, the following two conditions will ensure that $\dot{V}$ is negative semi-definite and hence a Lyapunov function:

$$m^{-1}M_t\sigma\delta^n - \alpha\dot{\tilde{k}}_e = 0 \tag{18}$$

and

$$m^{-1}M_t\sigma\delta^n\dot{\delta} - \beta\dot{\tilde{b}}_e = 0 \tag{19}$$

The adaptive laws for $\hat{k}_e$ and $\hat{b}_e$ can be directly derived from (18) and (19), respectively. They are computed as follows:

$$\dot{\tilde{k}}_e = \frac{m^{-1}M_t\sigma\delta^n}{\alpha} \tag{20}$$

$$\dot{\tilde{b}}_e = \frac{m^{-1} M_t \sigma \delta^n \dot{\delta}}{\beta} \tag{21}$$

Since $\tilde{k}_e = k_e - \hat{k}_e$ and k_e is a constant, then we have $\dot{\tilde{k}}_e = -\dot{\hat{k}}_e$. Likewise, $\dot{\tilde{b}}_e = -\dot{\hat{b}}_e$. These expressions can be used to re-write (20) and (21) as the following:

$$\dot{\hat{k}}_e = -\frac{m^{-1} M_t \sigma \delta^n}{\alpha} \tag{22}$$

$$\dot{\hat{b}}_e = -\frac{m^{-1} M_t \sigma \delta^n \dot{\delta}}{\beta} \tag{23}$$

Here, (22) and (23) represent the adaptation laws for $\hat{k}_e$ and $\hat{b}_e$, respectively. Since V is a valid Lyapunov function, we have therefore shown the boundedness of its states $\sigma, \tilde{k}_e, \tilde{b}_e$. Using Barbalat's lemma we can now show asymptotic convergence of Lyapunov function states.

B. Barbalat's Lemma

To apply Barbalat's Lemma and consequently show asymptotic convergence we must take the second derivative of our Lyapunov function and show that it is bounded. The second derivative is computed after plugging in (18) and (19) into (17) to obtain the following:

$$\ddot{V} = -2K\sigma\dot{\sigma} \tag{24}$$

We can substitute (11) and (12) into (24) to get a simplified expression:

$$\ddot{V} = -2K\sigma^2 + 2K\sigma m^{-1} M_t \tilde{F}_e \tag{25}$$

From the original Lyapunov analysis we know that σ is bounded along with the bounded constants K, m, and M_t. Since we assume that δ is bounded, and by construction of σ in (9), we also know that $\dot{\delta}$ is bounded. Since $\tilde{k}_e$ and $\tilde{b}_e$ are bounded from the original Lyapunov analysis, this shows that $\tilde{F}_e$ in (16) is also bounded. Therefore, every individual term in (25) is bounded, which implies that $\ddot{V}$ is also bounded. This satisfies Barbalat's Lemma and shows that the Lyapunov function state, σ, asymptotically converges to zero. Note, the states $\tilde{k}_e$ and $\tilde{b}_e$ have only shown to be bounded at this point.

C. Trajectory Generation

With σ converging to zero (which also implies e goes to zero as will be later shown), the objective now is to define an ideal reference trajectory, x_r^*, such that $F_e \to F_d$ as $x \to x_r^*$. In this way, as the robot tracks the reference trajectory, it will also track the desired force. This reference trajectory is computed by evaluating (4) in steady state, where all time derivatives are set to zero. This gives:

$$F_e = k_e \delta^n \tag{26}$$

By setting $F_e = F_d$ and substituting in the expression for δ we can re-write (26) as the following:

$$x_r^* = x_e + \left(\frac{F_d}{k_e}\right)^{\frac{1}{n}} \tag{27}$$

The computation of (27) is dependent on knowledge of the environment, k_e, which is unknown. Therefore, a feasible online trajectory, x_r, is derived by substituting the value of k_e with $\hat{k}_e$ to obtain the following:

$$x_r = x_e + \left(\frac{F_d}{\hat{k}_e}\right)^{\frac{1}{n}} \tag{28}$$

To achieve force tracking, the objective is to have $x_r \to x_r^*$. This is accomplished if $\hat{k}_e \to k_e$, which can alternately be stated as $\tilde{k}_e \to 0$. This will be shown later.

The expression for x_r in (28) is time-dependent due to the $\hat{k}_e$ term. The time derivative of x_r will be used in subsequent analysis and is computed as follows:

$$\dot{x}_r = -\frac{1}{n}\left(\frac{F_d \dot{\hat{k}}_e}{\hat{k}_e^2}\right)\left(\frac{F_d}{\hat{k}_e}\right)^{\frac{1-n}{n}} \tag{29}$$

D. Asymptotic Convergence of Error

As stated previously, the asymptotic convergence of σ does not necessarily imply asymptotic convergence of e in (9). However, with some manipulation this can also be shown. We start by recalling that $\dot{e} = \dot{x} - \dot{x}_r$, or alternatively $\dot{x} = \dot{e} + \dot{x}_r$. This expression along with (29) can be substituted into (9) to get the following:

$$\sigma = M_t \left[\dot{e} - \frac{1}{n}\left(\frac{F_d \dot{\hat{k}}_e}{\hat{k}_e^2}\right)\left(\frac{F_d}{\hat{k}_e}\right)^{\frac{1-n}{n}}\right] + B_t e \tag{30}$$

The expression in (22) can be substituted into (30) to obtain:

$$\sigma\left[1 - \frac{m^{-1} M_t^2 F_d \delta^n}{\alpha n \hat{k}_e^2}\left(\frac{F_d}{\hat{k}_e}\right)^{\frac{1-n}{n}}\right] = M_t \dot{e} + B_t e \tag{31}$$

With (31), we can see that every term within the square brackets has been previously shown to be bounded. This implies that the whole term in the square brackets is at least bounded, and that the left-hand-side of (31) goes to zero (since $\sigma \to 0$ due to Barbalat's lemma). Therefore the error dynamics equation can be simplified to the following:

$$0 = M_t \dot{e} + B_t e \tag{32}$$

This is a homogeneous differential equation in terms of e, which implies that $x \to x_r$ since $e \to 0$.

E. Asymptotic Convergence of $\tilde{k}_e$

After showing that $x \to x_r$, the last step is to show that $x_r \to x_r^*$, which would accomplish the force tracking task of $F_e \to F_d$. As previously stated, $x_r \to x_r^*$ if $\tilde{k}_e \to 0$. This is shown by starting with the impedance model found in (8). Through previous analysis we have shown that $\ddot{x}$, $\dot{e}$, and e will converge to zero. Additionally, it is apparent that the expression for γ in (12) will also converge to zero. Using these substitutions we obtain the following expression:

$$m^{-1} M_t \tilde{F}_e = 0 \tag{33}$$

Since m and M_t are both constants, this implies that $\tilde{F}_e$ will converge to zero. This can be used to rewrite (16) as follows:

$$\delta^n (\tilde{k}_e + \tilde{b}_e \dot{\delta}) = 0 \tag{34}$$

From the definition of σ in (9), we know that $\dot{\delta}$ converges to zero, and we are left with the following:

$$\delta^n \tilde{k}_e = 0 \tag{35}$$

The expression in (35) is equal to zero if either δ or $\tilde{k}_e$, or both, are equal to zero. Since we have shown that $x \to x_r$ we can guarantee that δ is a positive value as long as we assign F_d to be a value greater than zero. If δ remains positive then we know that $\tilde{k}_e$ must converge to zero to satisfy (35).

A note of significance is that although proper force tracking requires $\tilde{k}_e$ to converge to zero (which has been shown), it only requires $\tilde{b}_e$ to remain bounded (which has been shown using Lyapunov analysis). ■

V. Simulation

To verify the efficacy of the derived adaptive impedance controller, a 1-DOF robot interacting with a soft, viscoelastic environment is simulated. This simulation is akin to a palpation device used to interact with soft tissue in medical procedures, where constant force is applied to the tissue, e.g., to model a single jaw of a surgical robotic grasper or tissue retractor from the moment of first contact with tissue to a desired setpoint force that is most suitable for a specific tissue. Softer tissues typically require lower setpoint forces to avoid damage while stiffer tissues require higher setpoint forces to ensure traction, yet remain low enough to avoid excessive damage. Two distinct simulations were conducted with different material properties and desired force assigned for each trial. These simulations were performed using MATLAB's *ode45* solver with default settings invoking the parameters found in Table II. Trial A is akin to a softer tissue with a lower desired force target (e.g. kidney), and trial B is similar to a stiffer tissue with a higher desired force target (e.g. liver). The robot is modeled with mass, m, and damping, b. The tissue environment is modeled with the Hunt-Crossley model (2) with parameters k_e, b_e, and n. The desired dynamical relationship for the impedance controller is a 2^{nd} order mass-spring-damper with a target mass of M_t, target damping of B_t, and target spring constant of K_t. Other pertinent simulation parameters for the controller include gains α, β, and K. Additionally, the values were set for the environment location, x_e, and desired force, F_d. Initial location of the robot was set to be $x = 0.09$, and the initialization of $\hat{k}_e$ and $\hat{b}_e$ were set to be 75% of the true value.

TABLE II
Simulation Parameters

Parameter	Trial A	Trial B
m	1	1
b	0.05	0.05
k_e	50	400
b_e	10	20
n	1.8	1.8
M_t	1	1
B_t	2	2
K_t	1	1
α	$1.0e^{-7}$	$1.0e^{-7}$
β	$1.0e^{-5}$	$1.0e^{-5}$
K	25	25
x_e	0.1	0.1
F_d	1	2

VI. Results

The simulated results for trials A and B are shown in Figures 2 and 3, respectively. Each trial contains plots for position tracking, stiffness parameter estimation, and force tracking. The position tracking demonstrates the actual position, x, converging to the reference trajectory, x_r. This is the reference trajectory computed online by (28) which is designed to drive $F_e \to F_d$ so long as x_r converges to x_r^*.

The estimation of the stiffness parameter in the Hunt-Crossley model, $\hat{k}_e$, is shown to converge to the true value k_e for both trials.

The environment force, F_e is shown to converge to the desired force, F_d, for each trial. The environment force, F_e, is not accessible by the controller; instead, an estimate of the force, $\hat{F}_e$, can be computed based on the best current estimate of the environment parameters. For each trial, $\hat{F}_e$ very closely follows F_e, as is evident from the plots.

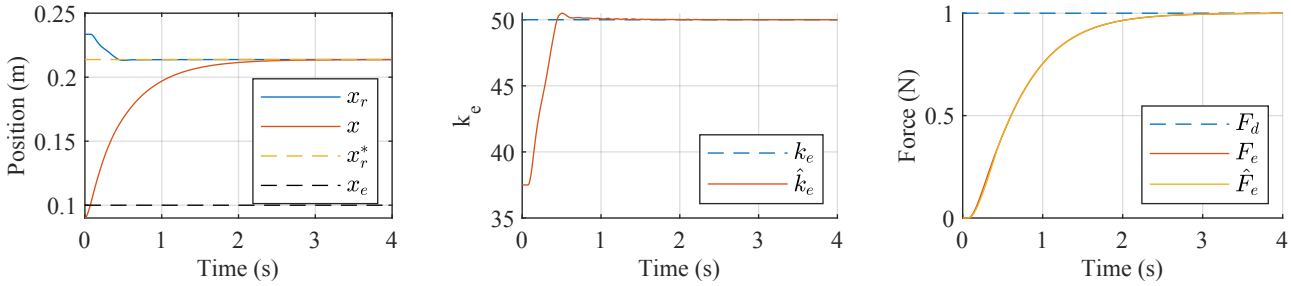

Fig. 2. Position tracking depicting convergence of x to both x_r and x_r^* (left), estimation of environment stiffness with $\hat{k}_e$ converging to the true value k_e (center), and force tracking of the environment force, F_e, converging to the desired force, F_d (right) for simulation trial A

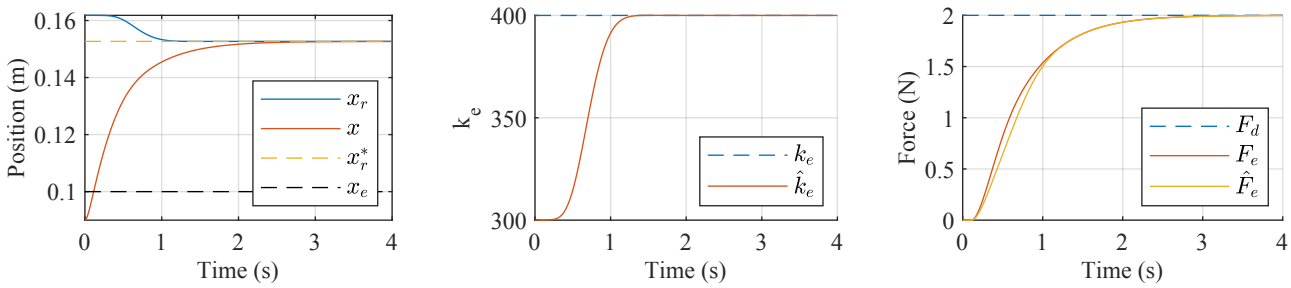

Fig. 3. Position tracking depicting convergence of x to both x_r and x_r^* (left), estimation of environment stiffness with $\hat{k}_e$ converging to the true value k_e (center), and force tracking of the environment force, F_e, converging to the desired force, F_d (right) for simulation trial B

VII. Discussion

The simulation results demonstrate accurate force tracking achieved with the proposed controller for both trials as depicted in Figures 2 and 3. This is achieved through proper assignment of a reference trajectory, x_r, as defined in (28). There are a few key observations to point out. First, F_d in (28) is a fixed value, i.e. the desired force is constant. Second, unlike a typical reference trajectory, which is computed independently of the system dynamics, the reference trajectory, x_r, in this framework depends on the environment parameter estimate, $\hat{k}_e$. This is because unlike a typical reference trajectory passed to a controller for motion tracking, our reference trajectory is also used for indirect force tracking. This makes position tracking more involved and it becomes crucial to have an increasingly better estimate of $\hat{k}_e$. Lastly, although initial investigation of time-varying force tracking in simulation has yielded promising results, it is left for future work to mathematically show stability in the presence of a time-varying desired force, F_d. The main challenge in accomplishing this is computing an expression for $\dot{x}_r$ in (29), which becomes much more complicated if F_d is not assumed to be constant. However, for many use cases a constant desired force will be sufficient (e.g. surgical grasping).

The key contribution this work provides is the implementation of a force tracking controller which does not rely on a force sensor or the computation of an acceleration term. This is significant as force sensors are generally expensive, and are often infeasible to add in many scenarios. This is specifically true in medical settings which is complicated because of sterilization issues as well as constraints due to small instrument size [16]. Additionally, the computation of a higher-order derivative, such as is necessary when computing acceleration, is noise-prone and undesirable in control loops because an accurate acceleration estimate incurs delay. The proposed work herein bypasses both of these concerns.

The current presentation of this work provides a solid foundation for further exploration. Currently, an estimation approach for the exponential term, n, is not included. This appears to be common in existing literature when estimation is used in conjunction with a controller. Fortunately, for soft tissue the value of n is generally bounded between 1 and 2, can easily be obtained offline, and is typically constant [3], [11].

VIII. Conclusion

This work presents an adaptive impedance controller for setpoint force tracking of robotic interactions with soft, viscoelastic materials. The controller is stable in both the free space and constrained space and stability is shown using Lyapunov analysis. Asymptotic stability is then shown by extending this analysis with Barbalat's lemma. Due to asymptotic convergence of position error, we are able to do force tracking (since x_r and F_d are intimately related using (28)). This is shown via the proof of the theorem presented in this work. The main advantages of this controller design include the ability to implement it without a force sensor or a computation of higher order dynamic terms such as acceleration. The simulation results demonstrate accurate force tracking for two distinct materials.

Future efforts to improve on this work include estimation of the coefficient, n, in the Hunt-Crossley model as well as force tracking of time-varying signals of F_d. The current work provides a foundation for further research to improve interaction with soft, viscoelastic materials such as interaction of robots with tissues for applications in medical robotics.

References

[1] N. Hogan, "Impedance control: An approach to manipulation: Part II–Implementation," *Journal of dynamic systems, measurement, and control*, vol. 107, no. 1, pp. 8–16, 1985.

[2] K. Hunt and F. Crossley, "Coefficient of restitution interpreted as damping in vibroimpact," *Journal of applied mechanics*, vol. 42, no. 2, pp. 440–445, 1975.

[3] A. Pappalardo, A. Albakri, C. Liu, L. Bascetta, E. De Momi, and P. Poignet, "Hunt–crossley model based force control for minimally invasive robotic surgery," *Biomedical Signal Processing and Control*, vol. 29, pp. 31–43, 2016.

[4] S. Jung, T. C. Hsia, and R. G. Bonitz, "Force tracking impedance control of robot manipulators under unknown environment," *IEEE Transactions on Control Systems Technology*, vol. 12, no. 3, pp. 474–483, 2004.

[5] H. Seraji and R. Colbaugh, "Force tracking in impedance control," *The International Journal of Robotics Research*, vol. 16, no. 1, pp. 97–117, 1997.

[6] K. Lee and M. Buss, "Force tracking impedance control with variable target stiffness," *IFAC Proceedings Volumes*, vol. 41, no. 2, pp. 6751–6756, 2008.

[7] W. Xu, C. Cai, M. Yin, and Y. Zou, "Time-varying force tracking in impedance control," in *Decision and Control (CDC), 2012 IEEE 51st Annual Conference on*. IEEE, 2012, pp. 344–349.

[8] S. Bhasin, K. Dupree, Z. Wilcox, and W. Dixon, "Adaptive control of a robotic system undergoing a non-contact to contact transition with a viscoelastic environment," in *American Control Conference, 2009. ACC'09*. IEEE, 2009, pp. 3506–3511.

[9] S. Bhasin, P. Patre, Z. Kan, and W. Dixon, "Control of a robot interacting with an uncertain viscoelastic environment with adjustable force bounds," in *American Control Conference (ACC), 2010*. IEEE, 2010, pp. 5242–5247.

[10] S. Bhasin, K. Dupree, P. M. Patre, and W. E. Dixon, "Neural network control of a robot interacting with an uncertain viscoelastic environment," *IEEE Transactions on Control Systems Technology*, vol. 19, no. 4, pp. 947–955, 2011.

[11] M. Hajimiri, H. A. Talebi, and M. Zareinejad, "Force tracking impedance control of robot-tissue interaction with a hunt-crosseley model," in *Control, Instrumentation, and Automation (ICCIA), 2016 4th International Conference on*. IEEE, 2016, pp. 142–147.

[12] N. Diolaiti, C. Melchiorri, and S. Stramigioli, "Contact impedance estimation for robotic systems," *IEEE Transactions on Robotics*, vol. 21, no. 5, pp. 925–935, 2005.

[13] A. Haddadi and K. Hashtrudi-Zaad, "Real-time identification of huntcrossley dynamic models of contact environments," *IEEE transactions on robotics*, vol. 28, no. 3, p. 555, 2012.

[14] R. Schindeler and K. Hashtrudi-Zaad, "Online identification of environment hunt–crossley models using polynomial linearization," *IEEE Transactions on Robotics*, vol. 34, no. 2, pp. 447–458, 2018.

[15] J. J. O'Neill, T. K. Stephens, and T. M. Kowalewski, "Evaluation of torque measurement surrogates as applied to grip torque and jaw angle estimation of robotic surgical tools," *IEEE Robotics and Automation Letters*, vol. 3, no. 4, pp. 3027–3034, 2018.

[16] P. Puangmali, K. Althoefer, L. D. Seneviratne, D. Murphy, and P. Dasgupta, "State-of-the-art in force and tactile sensing for minimally invasive surgery," *IEEE Sensors Journal*, vol. 8, no. 4, pp. 371–381, 2008.